JPP Journal of Pharmacy and Pharmacology

JPP 2007, 59: 373–381

Received August 29, 2006
Accepted November 22, 2006
DOI 10.1211/jpp.59.3.0006
ISSN 0022-3573

# Characterisation of blends of paracetamol and citric acid

Pekka Hoppu, Kirsi Jouppila, Jukka Rantanen, Staffan Schantz and Anne M. Juppo

## Abstract

The purpose of this study was to characterise physically stable amorphous blends that were sticky (low glass transition temperature) in ambient conditions. The effects of composition, melting time and melting temperature were evaluated with respect to physical and chemical property. Citric acid anhydrate and paracetamol were melt-quenched as binary mixtures and as pure materials. Bulk samples were characterised by differential scanning calorimetry, X-ray powder diffractometry, and Raman and Fourier transform infrared spectroscopy. The composition and the sample exposure to moisture affected significantly the physical stability of samples. The extreme melting conditions, coupled with long exposure to heat and a high melting temperature, lowered the overall crystallisation rate. Paracetamol had a stronger tendency to crystallise from the blends than did citric acid. The 50:50% (w/w) blend was physically stable for at least 27 weeks in dry conditions and was partly crystalline after 4 weeks of storage at a relative humidity of 43%. The result of the physical stability of blends is discussed in terms of hydrogen bonding interaction between paracetamol and citric acid and in relation to degradation products formed in a mixing state.

Faculty of Pharmacy, Division of Pharmaceutical Technology, P.O. Box 56, Fin-00014, University of Helsinki, Finland

Pekka Hoppu, Anne M. Juppo

Department of Food Technology, P.O. Box 66, Fin-00014, University of Helsinki, Finland

Kirsi Jouppila

Viikki Drug Discovery Technology Center DDTC, P.O. Box 56, Fin-00014, University of Helsinki, Finland

Jukka Rantanen

Department of Pharmaceutics and Analytical Chemistry, The Danish University of Pharmaceutical Sciences, DK-2100, Copenhagen, Denmark

Jukka Rantanen

AstraZeneca R&D, SE-431 83 Mölndal, Sweden

Staffan Schantz, Anne M. Juppo

**Correspondence:** P. Hoppu, Faculty of Pharmacy, Division of Pharmaceutical Technology, P.O. Box 56, Fin-00014, University of Helsinki. E-mail: pekka.hoppu@helsinki.fi

**Acknowledgments and Funding:** The authors gratefully acknowledge the financial support of AstraZeneca R&D Mölndal, and thank Mrs Maija Koljonen for carrying out the HPLC analysis.

## Introduction

An amorphous solid is characterised by a molecular short-range order, but without long-range order. An increasing number of research scientists are working with amorphous materials in pharmaceutical research and development (Yu 2001) due to advantages of the solid amorphous state over the crystalline state, and especially their dissolution properties. Typically, an amorphous solid exhibits a glass transition temperature ($T_g$) below which molecular translational motion is frozen. Factors that favour the formation of the glassy state are: a high viscosity in the liquid just above the solidification point, a rapid rate of cooling, a complex molecule structure and the presence of more than one molecular species (White & Cakebread 1966).

In the current literature, it is difficult to find an amorphous drug molecule that has a $T_g$ below room temperature in its dry state and that is physically stable at ambient conditions. Solid glass dispersions provide an opportunity to study small organic drug molecules that are normally physically unstable in the amorphous state as a pure substance in long-term storage. Timko & Lordi (1984) investigated several solid dispersions and the stability of these systems. The most stable material they found was a blend of citric acid anhydrate (CAA) and paracetamol at a 50:50% (w/w) ratio that was cooled from the melt. The $T_g$ (onset) of this system was 18°C and the blend was reported to be stable for at least seven weeks at 37°C under dry conditions. The complex showed no instability against mechanical and thermal handling.

The stability of amorphous citric acid is connected to the strong hydrogen bonding capacity. Timko & Lordi (1979) have even proposed that the decomposition products of CAA formed during melting may hinder the crystallisation process. It is also well known that paracetamol crystallises easily from the amorphous state (Di Martino et al 2000). The goal of this study was to characterise amorphous blends of CAA and paracetamol, having a low $T_g$ that favours glass–liquid transition at room temperature. The effect of different processing conditions on the properties of melt-quenched CAA and paracetamol as pure materials and as blends was tested systematically. The physical stability of the samples was evaluated on the molecular level using a range of analytical techniques. To study the possible

stabilising molecular interaction between paracetamol and CAA in the stable binary blends was one aim in this research. Large-scale processing studies require a cheap and physically stable system. Instead of a true drug substance of interest, which is sticky, amorphous, highly potent and expensive, the most stable blend of paracetamol and CAA will be used in further processing studies as a model substance.

## Materials and Methods

### Materials and design of experiment

CAA (USP) and paracetamol (USP) were purchased from Hawkins Inc. (Hawkins Inc., MN). Some physical properties of these molecules appear in Table 1 and the design of the experiments appears in Table 2. The factors included: composition of blend, melting temperature and melting time at constant temperature. The composition varied across five levels; all other factors varied across three levels. We performed a total of 28 tests with five duplicates.

### Melt-quenching and sampling

Compositions were melted in an electric heating reactor equipped with a temperature controlling system. The batch size was 50 g and the heating rate was $9 \pm 1$°C min$^{-1}$. Raw materials were inserted in the reactor at 100°C. The sample was then gently mixed by hand with a glass rod. The temperature was measured to an accuracy of ±2°C. The starting point of melting was defined as the time at which the composition reached the target temperature. The hot melt was poured onto two aluminium pans floating on liquid nitrogen and cooled within $60 \pm 10$ s to the final sample temperature of $20 \pm 10$°C. The sample thickness on the aluminium plate was $5 \pm 2$ mm.

### Aging study

Aluminium pans were inserted in desiccators (silica drying agent, relative humidity (r.h.) approx. 3%) to stabilise for 12 h. Samples were then characterised by high performance liquid chromatography (HPLC), Fourier transform infrared spectroscopy (FT-IR), X-ray powder diffraction (XRPD), Karl Fischer titration, differential scanning calorimetry (DSC) and Raman scattering.

Following this initial characterisation, one sample pan was exposed to 43% r.h. (desiccator with saturated aqueous $K_2CO_3$ solution, temperature approx. 23°C) and the other was placed in a dry silica desiccator. Samples in 43% r.h. were analysed at 1, 4, 8, 12 and 18 weeks after melting, whereas dry samples were analysed after 9, 18 and 27 weeks

**Table 1** Properties of paracetamol and CAA

| | Paracetamol | Citric acid anhydrate |
|---|---|---|
| Molecular structure | 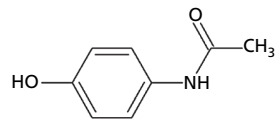 | 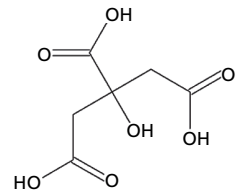 |
| Molecular weight | 151.2 g mol$^{-1}$ | 192.1 g mol$^{-1}$ |
| Melting point | 169°C | 153°C |
| $pK_a$ | 9.4 | 3.1; 4.8; 6.4 |
| Glass transition (onset) | 22.3°C[a] | 11°C[b] |
| Water solubility at 22°C | 0.1–0.5 g/100 mL | 10 g/100 mL |
| Hydrogen bond acceptors | -OH, C = O | -$OH_{alc}$, –$OH_{ac}$, C = O |
| Hydrogen bond donors | -OH, NH | -$OH_{alc}$, –$OH_{ac}$ |

[a]Di Martino et al (2000); [b]Lu & Zografi (1997).

**Table 2** Design of experiments

| Composition Paracetamol/CAA | Melting time 2 min | | | Melting time 6 min | | | Melting time 10 min | | |
|---|---|---|---|---|---|---|---|---|---|
| | 172°C | 179°C | 186°C | 172°C | 179°C | 186°C | 172°C | 179°C | 186°C |
| 0:1 | x + x | | x | | x | | x | | x |
| 1:3 | | x + x | | x | | x | | x | |
| 1:1 | x | | x | | x + x | | x | | x |
| 3:1 | | x | | x + x | | x | | x | |
| 1:0 | x | | x | | x | | x | | x + x |

23 tests = x, 5 duplicates = x + x.

with FT-IR, XRPD, Karl Fischer and Raman. All measurements were performed in triplicate (n = 3) except the ones with HPLC and XRPD (n = 1).

### High-performance liquid chromatography

The chemical stability of bulk samples was investigated using HPLC (Thermo Separation Products, San Jose, CA) equipped with a UV-VIS detector (model FOCUS, San Jose, CA). Wavelengths employed were 215 nm for CAA and 245 nm for paracetamol. The eluent used was composed of 96% (v/v) water with 0.1% (v/v) trifluoroacetic acid (TFA) at pH 2.1 and 4% (v/v) of acetonitrile. The injection size was 10 $\mu$L and the flow rate was 1 mL min$^{-1}$. We used an RP-18 column (150 × 4.6 mm, 5 $\mu$m) (Supelco, Bellafonte, PA).

### Karl Fischer titration

The amount of absorbed water was measured with a Mettler Toledo DL35 (Mettler-Toledo AG, Greifensee, Switzerland). Hydranal solvent (Riedel de Haën, Seelze, Germany) was used as a volumetric solvent and Hydranal titrant 5 as a volumetric titrant. The sample size was 100 ± 10 mg.

### Raman scattering

Raman spectra were acquired over the range 170–2200 cm$^{-1}$ with a Control Development spectrometer (Control Development Inc., South Bend, IN) equipped with a thermoelectrically cooled CCD detector and a fibre optic probe (RamanProbe; InPhotonics, Norwood, MA). We used a 500 mW laser source at 785 nm (Starbright 785S; Torsana Laser Technologies, Skodsborg, Denmark). The sample was rotated during measurement at approximately 30 rev min$^{-1}$. The integration time was 3 s. The median spectrum of these three spectra was constructed based on baseline and standard normal variate (SNV) transformation (Barnes et al 1989).

### Fourier transform infrared (FT-IR) spectroscopy

FT-IR spectra were measured over the spectral range 650–7500 cm$^{-1}$ with a Hyperion 1000 microscope (Bruker Optik GmbH, Ettlingen, Germany). The microscope was used to identify structures formed on the sample surface. Specular reflectance spectra were averaged from 64 scans at a resolution of 4 cm$^{-1}$. The Kramers-Kronig transformation was carried out using the software package provided (Opus 5.1; Bruker Optik GmbH, Ettlingen, Germany).

### Differential scanning calorimetry (DSC)

The glass transition temperature ($T_g$) of the bulk samples was measured with a Mettler TA 4000 DSC instrumented with a DSC-30 low temperature cell (Mettler-Toledo AG, Greifensee, Switzerland). Both onset (extrapolated) and midpoint values were determined. The nitrogen gas flow during measurements was 50 mL min$^{-1}$. The sample size was 9 ± 1 mg using 40 $\mu$L aluminium pans with a pinhole. The temperature ranged from −60°C to +100°C. Two scans were made for each sample at the same temperature range. The sample was held for 5 min at −60°C to stabilise the temperature before scans. The heating rate was 10°C min$^{-1}$ and the cooling rate was approximately 70°C min$^{-1}$.

In-situ melting was carried out by heating the samples in the DSC measuring cell to 170°C, 175°C and 180°C, after which instant cooling was performed. In addition, in-situ melting also took place at 179°C for 6 min. The heating rate was 10°C min$^{-1}$ in all the meltings. Blends were prepared with mortar and pestle before melting. Samples were measured with and without a pinhole. The $T_g$ was scanned once from −40°C to +50°C. The sample was held for 5 min at −40°C to reach the starting temperature. The cooling rate was approximately 70°C min$^{-1}$. One sample was measured at each temperature (n = 1), except at 170°C and 179°C, where we used at least two samples (n = 2 or n = 3).

### X-ray powder diffraction (XRPD)

An X-ray powder diffractometer was used to study the solid state of the samples (Bruker AXS D8 advance; Bruker AXS GmbH, Karlsruhe, Germany). The X-ray powder diffractometer was operated at 40 kV and 40 mA using CuK$\alpha$ radiation (1.54 Å). The diffraction angle varied from 10° to 40° ($2\theta$) with steps of 0.1° per 2 s. References to the crystalline structures of paracetamol and CAA, respectively, were taken from the Cambridge Structural Database (CSD; The Cambridge Crystallographic Data Centre, Cambridge, UK). The reference codes are HXACAN07 for monoclinic, and HXACAN08 for orthorhombic paracetamol (Nichols & Frampton 1998), and CITRAC10 for CAA, and CITARC for citric acid monohydrate (Glusker et al 1969; Roelofsen & Kanters 1972). The structures and X-ray powder diffraction patterns of paracetamol and citric acid were visualised and calculated with Mercury 1.4.1 software (CCDC 2001–2005, Cambridge, UK).

### Statistical methods

Design of experiments (DOE) and data analysis were made by Modde version 7.0 (Umetrics AB, Umeå, Sweden) with multilinear regression method. Spectral and DSC data were evaluated with multivariate data analysis using projection method, with a Simca-P version 10.5 (Umetrics AB, Umeå, Sweden). The design of experiment was a full factorial-interaction model with a total of 45 experiments (+duplicates), which were reduced to 28 experiments (23 tests + 5 duplicates). In DSC thermogram, Raman and FT-IR spectra the median one of three measured spectra was selected and presented in the figures.

## Results

### Effect of melting method on glass transition temperature

*In-situ melting in the DSC pan*

The results of in-situ melting appear in Table 3. The standard deviations of measurements varied from 0.5°C to 1.4°C, and were the highest in the onset values. Pure paracetamol samples, melted at 170 and 175°C, crystallised during cooling. In

**Table 3** Effect of composition and melting conditions on $T_g$ values. The onset ($T_g^o$) and the midpoint ($T_g^{mid}$) value

| Melting | 170°C for 10 s | | | | 175°C for 10 s | | | | 180°C for 10 s | | | | 179°C for 6 min | |
|---|---|---|---|---|---|---|---|---|---|---|---|---|---|---|
| Composition of paracetamol | Without pinhole | | With pinhole | | Without pinhole | | With pinhole | | Without pinhole | | With pinhole | | Without pinhole | With pinhole |
| | $T_g^o$ | $T_g^{mid}$ | $T_g^o$ | $T_g^{mid}$ | $T_g^o$ | $T_g^{mid}$ | $T_g^o$ | $T_g^{mid}$ | $T_g^o$ | $T_g^{mid}$ | $T_g^o$ | $T_g^{mid}$ | $T_g^o$ | $T_g^o$ |
| 0% | 8.1 | 11.7 | 10.0 | 13.6 | 7.7 | 11.3 | 10.6 | 14.2 | 6.6 | 10.3 | 11.4 | 15.0 | 4.2 | 13.9 |
| 25% | 7.4 | 13.9 | 9.0 | 17.3 | 4.9 | 10.8 | 9.0 | 18.5 | 2.7 | 8.5 | 10.5 | 18.1 | −8.3 | 10.3 |
| 50% | 11.8 | 17.6 | 13.9 | 21.5 | 10.5 | 15.9 | 14.8 | 22.8 | 7.2 | 12.3 | 17.5 | 23.7 | −7.0 | 17.2 |
| 75% | 17.6 | 21.3 | 22.5 | 26.3 | 16.3 | 20.2 | 21.4 | 25.7 | 11.2 | 15.4 | 20.3 | 25.1 | 1.8 | 18.8 |
| 100% | —* | —* | —* | —* | —* | —* | —* | —* | 22.0 | 25.0 | 22.2 | 25.1 | 21.7 | 22.4 |

*Crystals.

all the other DSC experiments, we detected a single, more or less composition-dependent glass transition for the blends, regardless of the processing conditions. We noticed significant differences for samples measured with or without a pinhole. With a pinhole, volatile products may evaporate at higher temperatures during the DSC scan. $T_g$s measured with a pinhole were higher than those measured without a pinhole. In the latter case (melting at 179°C for 6 min), binary mixtures showed approximately 20°C lower $T_g$s than those reported in the literature. Measured $T_g$ values decreased as the melting temperature increased or as the melting time increased.

*Bulk samples*

The blend samples were slightly yellowish and transparent after the melting. Pure CAA samples were slightly opaque with minor white colour. The pure paracetamol samples were opaque with white or pink colour, depending on the melting conditions. A single glass transition was detected for all the blends, as well as pure CAA. Pure paracetamol samples had crystallised. Onset values rose with correspondingly higher amounts of paracetamol from 13.9°C to 20.5°C (using pan with a pinhole) in the first scan and from 8.7°C to 16.8°C in the second scan (Figure 1). The poor contact between the sample and the DSC pan may have disturbed the measurement in the first scan because the samples were sticky, and good thermal transfer may not have been attained. Midpoint values varied similarly from 18.1°C to 24.9°C in the first scan and from 14.0°C to 21.3°C in the second scan. The onset values showed a standard deviation from 0.8°C to 1.3°C (min–max), and for the midpoint values, the standard deviation varied from 0.9°C to 1.7°C. We recorded an exothermic peak for pure CAA at 65°C, and the 75% paracetamol blend at 75°C.

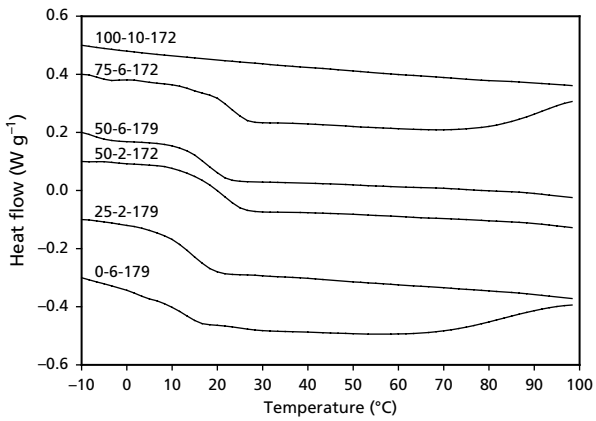


**Figure 1** Glass transitions of bulk samples from the second scan of DSC analysis. Label symbols: amount of paracetamol (w/w %)-melting time (min)-melting temperature (°C).

*HPLC of bulk samples*

Pure paracetamol was 97% pure regardless of melting temperature and melting time. More degradation occurred in the pure CAA samples. Some of the degradation products of CAA may have eluted at the same time as CAA due to short elution time resulting in the underestimation of the degradation products. The low temperature of 172°C produced less than 5% of the degradation products in CAA, regardless of the melting time. No extra peaks were detected in the pure paracetamol samples and only one extra peak was detected in pure CAA samples.

In the blends, the purity of paracetamol was 84–97% (min–max). Paracetamol was less stable in the composition containing 25% paracetamol. Similarly for CAA, the estimated purity was 17–98% in the blends. Minimum values for CAA were detected from the samples containing 75% paracetamol. In the blend samples, three extra peaks were detected in addition to the CAA and paracetamol peaks. Generally, long melting time and high melting temperature increased the amount of degradation products in all the samples. The loss of any small organic degradation products due to open heating conditions might have altered the composition ratio. The sample 50-2-172 had a purity of 87% while the sample 50-10-172 had a purity of 55% CAA. The purity of paracetamol exceeded 95% in these systems.

## Aging study in dry conditions and at 43% r.h.

*Determination of moisture content*

The moisture content of raw materials was 0.02% for paracetamol and 0.13% for CAA, but higher for processed samples (n = 3) (Table 4). Crystallised pure paracetamol samples showed the lowest moisture content. The high amount of

**Table 4** The moisture content of samples after different storage times under different conditions

| **Storage humidity (r.h.)** | **3%** | **43%** | **43%** | **43%** | **43%** | **43%** |
|---|---|---|---|---|---|---|
| Amount of paracetamol (w/w) | 12 h | 1 week | 4 weeks | 8 weeks | 12 weeks | 18 weeks |
| 0% | 1.8 ± 0.5 | 2.0 ± 0.7 | 4.2 ± 1.5 | 4.4 ± 1.3 | 3.6 ± 1.5 | 4.1 ± 1.0 |
| 25% | 2.0 ± 1.0 | 4.5 ± 1.8 | 8.2 ± 2.0 | 6.2 ± 1.7 | 5.5 ± 1.6 | 4.7 ± 1.5 |
| 50% | 1.5 ± 0.5 | 2.6 ± 0.8 | 4.7 ± 1.0 | 4.1 ± 0.9 | 4.2 ± 0.8 | 4.3 ± 1.2 |
| 75% | 1.2 ± 0.2 | 2.0 ± 0.4 | 2.3 ± 0.5 | 2.5 ± 0.7 | 2.6 ± 0.5 | 2.4 ± 0.3 |
| 100% | 0.2 ± 0.1 | 0.2 ± 0.1 | 0.2 ± 0.1 | 0.1 ± 0.1 | 0.1 ± 0.1 | 0.1 ± 0.1 |

Data are means ± s.d.

CAA in the blend sample increased the moisture content of the sample. After four weeks' storage, the moisture content of the 25% paracetamol blend sample decreased due to crystallisation at 43% r.h. Samples held in the silica desiccator exhibited a moisture content of 0.6 ± 0.5 after 18 weeks' storage.

*XRPD*

The XRPD diffractograms and proposed crystal structures appear in Figures 2–4 (n = 1). Only a few weak diffractions were observed in the pure CAA samples, whereas pure paracetamol had crystallised after 12 h storage in dry conditions (Figure 2). All the other blend samples showed a broad halo in the diffractograms, thus confirming their amorphous states. Pure paracetamol had crystallised into the monoclinic form as the characteristic peaks show. Peaks in CAA corresponded to the anhydrate form. We compared the molecular structure of CAA (measured by Glusker et al (1969)) to XRPD data and observed the highest XRPD intensities of pure CAA at 16.5° and 19.5°, which were assigned the Bragg reflection values of (002) (Miller Index) and (201), respectively (Figure 3). In the vertical (002) and longitudinal direction (201), a carboxylic group dimerisation is crucial in these planes.

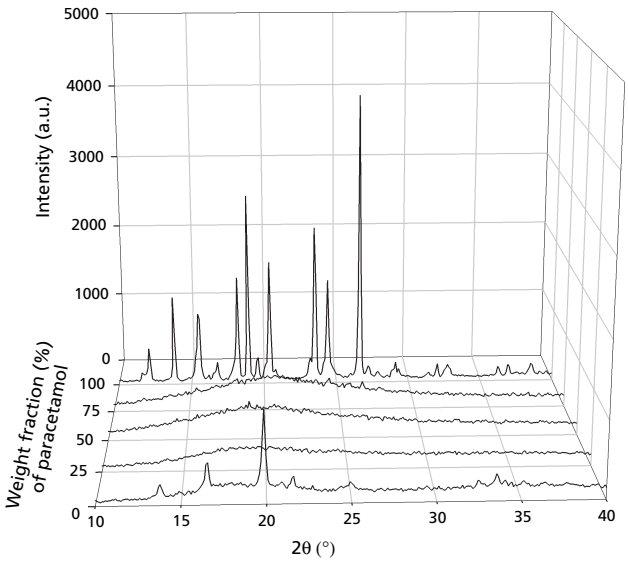


**Figure 2** XRPD diffractograms of paracetamol, CAA and their blend samples stored for 12 h at 3% r.h. after melt processing.

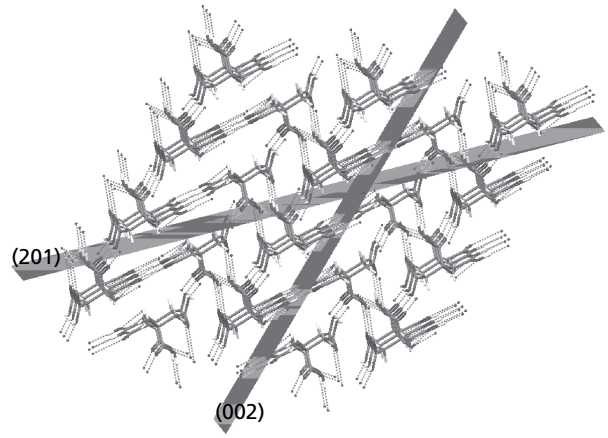


**Figure 3** Bragg reflection plane (002) and (201) in CAA, corresponding to the 2$\theta$ reflection at 16.5° and 19.5°, respectively.

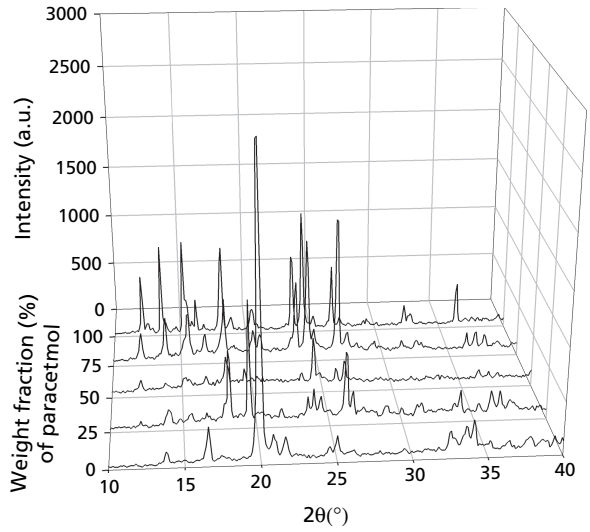


**Figure 4** XRPD diffractograms of paracetamol, CAA and their blend samples stored for 12 weeks at 43% r.h. after melt processing.

*Storage at 43% r.h.*

Samples containing 75% paracetamol exhibited clear XRPD peaks characteristic for monoclinic paracetamol and revealing crystallisation within a week. For the samples rich in CAA, crystallisation had also occurred with some peaks at

diffraction angles similar to pure crystalline CAA. After four weeks of storage, the 25% and 50% of paracetamol compositions were partly crystalline, including the 50% blend that showed in diffractograms with weak similarities to that of monoclinic paracetamol. Samples melted at extreme conditions showed lower intensities (only a few peaks with weak intensities) than did those that underwent gentle melting procedure (short time, low temperature). Over time, XRPD peak intensities increased as expected. Monoclinic paracetamol appeared to dominate diffractograms for samples containing 50% or more paracetamol, whereas the composition containing 25% paracetamol resembled a physical mixture of CAA and paracetamol (Figure 4).

*Storage in dry conditions*

All blend samples stored for 27 weeks in dry conditions appeared amorphous, evinced by a broad halo in its XRPD spectrum. We detected peaks only for samples containing pure paracetamol or pure CAA. We confirmed the crystals to be CAA and monoclinic paracetamol.

*FT-IR spectroscopy*

In the intermediate frequency region, we detected the C=O stretching of pure CAA at approximately at 1700 $cm^{-1}$ (Figure 5, line g). Dimerisation usually occurs in the C=O stretching in the range 1690–1720 $cm^{-1}$. The peak, starting at wavenumber 1740 $cm^{-1}$ and higher (Figure 5, line h), was connected to the OH stretching, lowered due to hydrogen bonding (Rao & Narayanaswamy 1970). The skeletal vibrational modes at the band area ranging from 1100 $cm^{-1}$ to 1400 $cm^{-1}$ is complicated to analyse in detail due to many different $CH_2$ and carboxyl group deformations and stretchings.

Samples containing 75% or 100% paracetamol produced the same form as did original monoclinic paracetamol. In the monoclinic paracetamol form, C=O stretching occurred at approximately 1654 $cm^{-1}$ (Burgina et al 2004) (Figure 5, line f). The peaks in the 1650–1500 $cm^{-1}$ region are from the stretching of the aromatic ring combined with deformation of the amide group. The peak located at 1610 $cm^{-1}$ is connected with the stretching of the aromatic ring (Figure 5, line e). Peaks at 1565 and 1510 $cm^{-1}$ are combination bands of phenol stretching and of deformation of the CNH group (Figure 5, lines c and d). The peak at 1442 $cm^{-1}$ is the combination band of phenol stretching and deformation of the $CH_3$ group (Figure 5, line b).

In the amorphous form of the 25% and 50% blends, only one broad peak occurred at approximately 1700 $cm^{-1}$ (Figure 5, line g). The OH stretching band (Figure 5, line h) had vanished or merged with the C=O stretching band. Similar behaviour occurred at the band area around 1200 $cm^{-1}$ (Figure 5, line a), where all the peaks had merged together into a single broad band. The band at 1510 $cm^{-1}$ appeared at approximately the same frequency as in the crystalline paracetamol form (Figure 5, line c). Peaks at 1654, 1610 and 1565 $cm^{-1}$ had broadened or merged with other bands (Figure 5, lines d, e, f). The peak at 835 $cm^{-1}$ is the out-of-plane vibration of phenyl C-H groups and has occurred with greater intensity in the orthorhombic form than in the monoclinic form of paracetamol (Moynihan & O'Hare 2002). In the amorphous 50:50% blend, this band was more intense than in the monoclinic paracetamol form.

All amorphous samples with no crystals merged into a broad band at 2500–3600 $cm^{-1}$ with no distinguishable peaks. In the crystallised pure CAA sample, the broad band ranging from 2500 $cm^{-1}$ to 3600 $cm^{-1}$ narrowed and we detected some fine structure. This is typical behaviour for carboxylic acids. The monoclinic paracetamol showed peaks at 3161 $cm^{-1}$ and 3327 $cm^{-1}$ (Burgina et al 2004). The pure CAA sample showed characteristic peaks of crystalline CAA at 3277 $cm^{-1}$ and 3485 $cm^{-1}$ (Rao & Narayanaswamy 1970).

After one weeks' storage at 43% r.h., all the samples displayed surface crystals. Samples containing 0% and 25% paracetamol showed characteristic peaks of crystalline CAA. For all the other samples, we found peaks of crystalline paracetamol. The sample containing 75% paracetamol produced characteristic peaks of both orthorhombic and monoclinic paracetamol. For longer storage times, we detected only the monoclinic paracetamol form. After four weeks' storage at 43% r.h., the sample containing 25% paracetamol showed both CAA and paracetamol crystals. Similarly, a few CAA crystals formed in the sample with 50% paracetamol. In the sample with 75% paracetamol, we identified only paracetamol crystals.

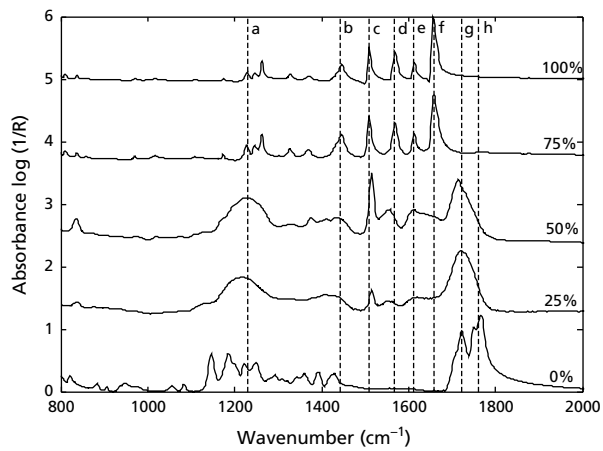


**Figure 5** FT-IR specular reflectance spectra (corrected with the Kramers-Kronig transformation) of samples maintained in a silica desiccator for 18 weeks. Amount of paracetamol (w/w %), as indicated at right.

*Raman scattering*

Bands of paracetamol from 1350 to 1180 $cm^{-1}$ represent combinations of C-H deformation and N-H bendings (Pestaner et al 1996) (Figure 6). The C=O peak at 1649 $cm^{-1}$, the N-H deformation mode at 1620 $cm^{-1}$, and the H-N-C=O stretching mode at 1562 $cm^{-1}$ were all well recognised from the crystalline paracetamol sample (Figure 6, lines i, h, g). These bands merged together or formed a broad peak in the amorphous blends. C-H deformations and phenol group deformation usually occurred at 1184 $cm^{-1}$ (Colthup et al 1975) (Figure 6, line d), but shifted to a slightly higher wavenumber in the amorphous blends. The band at 865 $cm^{-1}$ represents the out-of-plane vibration of the phenyl group, and also shifted to a slightly higher wavenumber (Figure 6, line a).

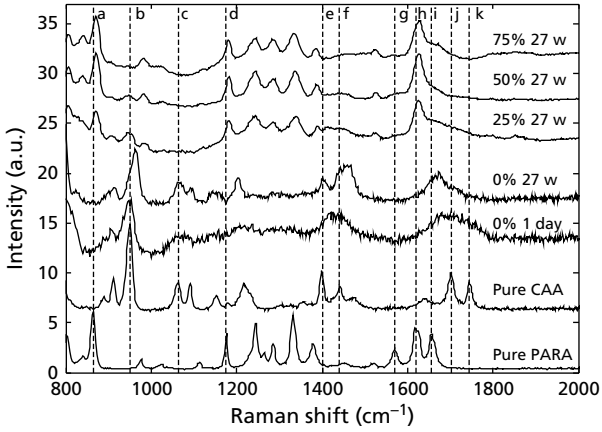


**Figure 6** SNV and baseline-corrected Raman spectra of raw materials of paracetamol (PARA) and CAA and their blends stored for 1 day or 27 weeks under dry conditions. Labels indicate the amount of paracetamol (w/w %) and storage time (1 day or 27 weeks).

Bands of crystalline CAA at 1700 and 1736 $cm^{-1}$ are connected to C = O and –OH stretching (Tarakeshwar & Manogaran 1994) (Figure 6, lines j and k). In molten CAA, reported peaks occurred at 418, 870, 1071, 1442, 1739 and 2984 $cm^{-1}$ (von Thatte & Askhedkar 1936) and are connected to O-C = O group motions, and bands at approximately 1400 $cm^{-1}$ approach deformation frequencies of $–CH_2$ (Tarakeshwar & Manogaran 1994) (Figure 6, lines e and f). The peaks detected in the crystalline form at 1000–1100 $cm^{-1}$ disappeared in the amorphous samples, but could be distinguished later in pure CAA after 27 weeks' storage under dry conditions. These resonances are connected to the deformation of COO and $CH_2$ (Tarakeshwar & Manogaran 1994) (Figure 6, line c). Under humid conditions, similar peaks formed after four weeks' storage at 43% r.h.. For all the samples, as the material crystallised under humid conditions, the peak intensity increased and the baseline decreased. Samples containing 25% paracetamol produced a characteristic CAA peak at 943 $cm^{-1}$, which represents the C-OH bending vibration (Tarakeshwar & Manogaran 1994) (Figure 6, line b).

## Discussion

### Effect of melting on glass transition temperature

As expected for miscible single phase blend, a higher paracetamol content in the blends raised the onset and the midpoint values (Figure 1). A long melting time and a high melting temperature in the melting process shifted the onset and the midpoint ($T_g$) values to slightly lower temperatures in relation to the higher supported amounts of degradation products formed, especially in the in-situ measurement without a pinhole (Table 3). This was supported by the results from the HPLC analysis of the bulk samples.

CAA seemed sensitive to degradation, and paracetamol accelerated the degradation of CAA as the $T_g$ values of the samples containing 25% paracetamol show (Table 3). One of the known degradation products is water, which acts as a plasticiser. Water is known to be difficult to remove from citric acid melts and lowers $T_g$ (Summers & Enever 1980). The degradation products of CAA may evaporate through a pinhole and may thus increase the observed $T_g$ values of blends. Significantly, the degradation of CAA may also alter the ratio between CAA and paracetamol (i.e. raise the paracetamol content) in the blends, favouring higher $T_g$ values. The batch size also affected the degradation products because the yield of itaconic anhydride, for example, decreased in larger runs (Shriner et al 1931b). Possible degradation products for the CAA at processing temperatures used are itaconic anhydride (melting point (mp) 66°C, boiling point 114°C), itaconic acid (mp 165°C) and aconitic acid (mp 190°C) (Shriner et al 1931a, b; Timko & Lordi 1982). Paracetamol is reported to be relatively stable against heat in its dry state (Fairbrother 1974).

### Effect of composition on physical stability

The composition was one of the most significant factors influencing physical stability. Paracetamol crystallised more easily than did CAA. CAA is known to nucleate rapidly, but after this initial stage, the crystallisation rate decreased, likely due to rearrangement of the small crystals (Timko & Lordi 1979). As shown by Raman and XRPD, the crystallisation process for CAA was slow under dry conditions. Pure CAA and the sample containing 75% paracetamol were thermally unstable in the bulk samples and they already began to crystallise during the DSC scan at 65°C and at 75°C, respectively (Timko & Lordi 1979; Di Martino et al 2000). This phenomenon was related to a small nucleus in the samples that favour crystallisation. The binary mixtures were physically more stable than the pure samples. The most physically stable composition was the 50:50% blend. This might be the result of a favourable blend ratio to stabilise molecular interactions. Also, the high viscosity of the 50:50% melt after pouring onto the aluminium pan may have contributed to the decrease in nucleation, thus favouring the slow crystallisation of the blend sample. In the HPLC analysis, the pure materials were more stable against heat and a long melting time than were the binary mixtures.

### Effect of melting time and melting temperature on physical stability

Tougher blend processing (i.e. high melting temperature, long melting time) resulted in a lower degree of overall crystallinity. Crystals were still detected in all the samples by XRPD, Raman, FT-IR and visual inspection – especially at 43% r.h. – regardless of melting time and melting temperature. Apparently, to avoid the significant degradation of CAA, as in the in-situ $T_g$ measurements, the melting temperature should not exceed 175°C. In addition, the melting time should be as short as possible to avoid any excess thermal energy. The nucleation of CAA and paracetamol was somewhat slower for samples with a higher content of degradation products, which may have hindered nucleation. Hendriksen et al (1998) reported that the nucleation process

of paracetamol, for example, can be disturbed by structurally related substances.

### Molecular interactions and physical stability

The broadness of the peaks in FT-IR and Raman spectra resulted from a wider distribution of the inter-molecular structures. In addition, due to changes in hydrogen bonding, some bands shifted or merged with other bands. Wang et al (2002) have reported the broadening and peak shifting of C=O, O-H and N-H bands in pure amorphous paracetamol and Nair et al (2001) the same for the paracetamol blends. In the amorphous blends, small shifts of the phenyl ring vibration in the Raman scattering spectrum may also indicate differences in the short-range contacts (Van der Waals forces). The phenyl ring structure is thought to help to stabilise amorphous paracetamol through stabilising the intermolecular interactions such as dipole forces (Timko 1979).

Dimerisation is common for carboxylic acids and dimer formation has been mentioned as a prerequisite to indometacin crystal formation from the amorphous state (Taylor & Zografi 1997). Steiner (2002) mentioned that engineering with carboxylic acid dimers requires the absence of other hydrogen-bond competitors. It is speculated that paracetamol disturbs the dimerisation of CAA, as the XRPD data of pure CAA indirectly show (Figure 3). Similarly, hydrogen bonds between paracetamol and CAA appeared to compete with hydrogen bonds characteristic of pure substance components. Paracetamol is known to form hydrogen bonds with other molecules – in some cases even forming co-crystals (Oswald et al 2002) – if not hindered by steric effects. Timko (1979) reported that –OH and –NH-C=O-$CH_3$ groups are important in paracetamol glass formation, and these groups can also disrupt the dimerisation of CAA by hydrogen bonding.

It was found that the crystallisation rate at 43% r.h. was faster than under dry conditions. Water, being an extremely potent hydrogen-bond competitor in carboxylic acids, may break or disrupt hydrogen bonds between paracetamol and CAA. This allows molecules to re-orientate and favour the crystallisation of these materials. Crystallisation, in particular, appeared faster on the surface of the samples due to water absorption and plasticisation of the surface. In protein studies, more water is reported to bind directly to C=O than to N-H groups (Baker & Hubbard 1984). In addition, –OH groups also attract water molecules. Thus, water may bind mainly to CAA because of the higher number of OH and C=O groups. This was seen in the Karl Fischer results, where the amorphous blends with high CAA content contained the most water. The crystallinity of CAA reduced its water content because crystalline material can bind water only on the surface of crystals (with the exception of hydrates), while an amorphous material can hydrogen-bond water also internally (Bell & Labuza 2000).

### Conclusions

The 50:50% blend formed the most stable physical blend for further processing. Mixing CAA and paracetamol disturbed the hydrogen bonding between similar species, thus favouring the formation of an amorphous blend. FT-IR and XRPD results, in particular, detected less frequently the dimerisation of carboxylic acid group of CAA. This was the result of the competitive hydrogen bonding of paracetamol with CAA. Hydrogen-bond interactions with CAA and paracetamol were stronger in the blend than with similar molecules. Water increased the crystallisation rate of amorphous blends due to its plasticisation properties.

Pure materials and the blend containing 75% paracetamol were thermally unstable and already crystallised during DSC scanning. At room temperature, CAA and paracetamol crystallised as pure substances from the blends. Monoclinic paracetamol crystals formed within the range 25–100% paracetamol, and CAA crystals were formed within the range 0–50% paracetamol after 4 weeks' storage at 43% r.h. Under dry conditions as measured by XRPD, all the blends remained amorphous after 27 weeks' storage. Chemical degradation depended on composition and melting parameters. To avoid excess chemical degradation during melting, the processing temperature should not exceed 175°C and the melting time should be kept as short as possible. Degradation products decreased the measured $T_g$s, especially if closed pans are used. Degradation products may have contributed to the lower crystallisation rate.

## References


Baker, E. N., Hubbard, R. E. (1984) Hydrogen bonding in globular proteins. *Prog. Biophys. Mol. Biol*. **44**: 97–179

Barnes, R. J., Dhanoa, M. S., Lister, S. J. (1989) Standard normal variate transformation and de-trending of near-infrared diffuse reflectance spectra. *Appl. Spectrosc*. **43**: 772–777

Bell, L. N., Labuza, T. P. (2000) *Moisture sorption. Practical aspects of isotherm measurement and use*. The American Association of Cereal Chemists Inc., USA

Burgina, E. B., Baltakhinov, V. P., Boldyreva, E. V., Shakhtscheiner, T. P. (2004) IR spectra of paracetamol and phenacetin. 1. Theoretical and experimental studies. *J. Struct. Chem*. **45**: 64–73

Colthup, N. B., Daly, L. H., Wiberly, S. E. (1975) *Introduction to infrared and Raman spectroscopy*. Academic Press, New York, USA

Di Martino, P., Palmieri, G. F., Martelli, S. (2000) Molecular mobility of the paracetamol amorphous form. *Chem. Pharm. Bull*. **48**: 1105–1108

Fairbrother, J. E. (1974) Acetaminophen. In: Florey, K. (ed.) *Analytical profiles of drug substances*. Academic Press, New York, USA, pp 2–109

Glusker, J. P., Minkin, J. A., Patterson, A. L. (1969) X-ray crystal analysis of the substrates of aconitase. IX. A refinement of the structure of anhydrous citric acid. *Acta Crystallogr. B* **25**: 1066–1072

Hendriksen, B. A., Grant, D. J. W., Meenan, P., Green, D. A. (1998) Crystallisation of paracetamol (acetaminophen) in the presence of structurally related substances. *J. Cryst. Growth* **183**: 629–640

Lu, Q., Zografi, G. (1997) Properties of citric acid at the glass transition. *J. Pharm. Sci*. **86**: 1374–1378

Moynihan, H. A., O'Hare, I. P. (2002) Spectroscopic characterisation of the monoclinic and orthorhombic forms of paracetamol. *Int. J. Pharm*. **247**: 179–185

Nair, R., Nyamweya, N., Gonen, S., Martinez-Miranda, L. J., Hoag, S. W. (2001) Influence of various drugs on the glass transition temperature of poly(vinylpyrrolidone): a thermodynamic and spectroscopic investigation. *Int. J. Pharm*. **225**: 83–96

Nichols, G., Frampton, C. S. (1998) Physicochemical characterization of the orthrorombic polymorph of paracetamol crystallized from solution. *J. Pharm. Sci*. **87**: 684–693

Oswald, I. D. H., Allan, D. R., McGregor, P. A., Motherwell, W. D. S., Parsons, S., Pulham, C. R. (2002) The formation of paracetamol (acetaminophen) adducts with hydrogen bond acceptors. *Acta Crystallogr. B* **58**: 1057–1066

Pestaner, J. P., Florabel, M. D., Mullick, M. D., Centeno, J. A. (1996) Characterization of acetaminophen: molecular microanalysis with Raman microprobe spectroscopy. *J. Forensic Sci*. **41**: 1060–1063

Rao, M. K., Narayanaswamy, C. K. (1970) Infrared spectrum of anhydrous citric acid in the solid state. *Indian J. Phys*. **44**: 34–38

Roelofsen, G., Kanters, J. A. (1972) Citric acid monohydrate. *Cryst. Struct. Comm*. **1**: 23–26

Shriner, R. L., Ford, S. G., Roll, L. J. (1931a) Itaconic anhydride and itaconic acid. *Org. Synth*. **11**: 70

Shriner, R. L., Ford, S. G., Roll, L. J. (1931b) Citraconic anhydride and citraconic acid. *Org. Synth*. **11**: 28

Steiner, T. (2002) The hydrogen bond in the solid state. *Angew. Chem. Int. Ed. Engl*. **41**: 48–76

Summers, M. P., Enever, R. P. (1980) Glass transition temperature of citric acid. *J. Pharm. Sci*. **69**: 612–613

Tarakeshwar, P., Manogaran, S. (1994) Ground state vibrations of citric acid and the citrate trianion: an ab initio study. *Spectrochim. Acta Part A* **50**: 2327–2343

Taylor, L. S., Zografi, G. (1997) Spectroscopic characterization of interactions between PVP and indomethacin in amorphous molecular dispersions. *Pharm. Res*. **14**: 1691–1698

Timko, R. J. (1979) *Thermal characterization of glass dispersion sysytems*. Rutgers, The state university of New Jersey, New Brunswick

Timko, R. J., Lordi, N. G. (1979) Thermal characterization of citric acid solid dispersions with benzoic acid and phenobarbital. *J. Pharm. Sci*. **68**: 601–605

Timko, R. J., Lordi, N. G. (1982) The effect of thermal history on the transition temperature of citric acid glass. *J. Pharm. Sci*. **71**: 1185–1186

Timko, R. J., Lordi, N. G. (1984) Thermal analysis of glass dispersion systems. *Drug Dev. Ind. Pharm*. **10**: 425–451

von Thatte, V. N., Askhedkar, D. Y. (1936) Raman-Spektren einiger organischer Säuren und ihrer Derivative im geschmolzenen Zustande. *Z. Physik* **100**: 456–462

Wang, S.-L., Lin, S.-Y., Wei, Y.-S. (2002) Transformation of metastable forms of acetaminophen studied by thermal fourier transform infrared (FT-IR) microspectroscopy. *Chem. Pharm. Bull*. **50**: 153–156

White, G. W., Cakebread, S. H. (1966) The glassy state in certain sugar-containing food products. *J. Food Technol*. **1**: 73–82

Yu, L. (2001) Amorphous pharmaceutical solids: preparation, characterization and stabilization. *Adv. Drug Del. Rev*. **48**: 27–42